ACS APPLIED MATERIALS & INTERFACES

RESEARCH ARTICLE

www.acsami.org

A Substrate-Independent Lift-Off Approach for Patterning Functional Surfaces

P. S. Brown, T. J. Wood, W. C. E. Schofield, and J. P. S. Badyal*

Department of Chemistry, Science Laboratories, Durham University, Durham DH1 3LE, England, United Kingdom

ABSTRACT:

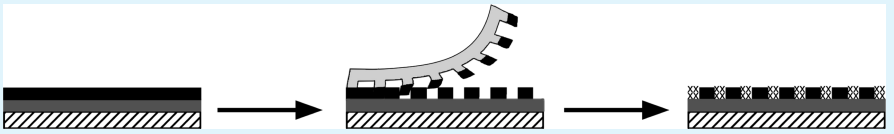

A lift-off method for creating multifunctional patterned surfaces has been devised. It entails consecutive pulsed plasmachemical deposition of a reactive bottom layer and a protective top release layer. By way of example, a bottom/top layer combination comprising pulsed plasma deposited poly(glycidyl methacrylate)/poly(pentafluorostyrene) has been shown to display selective adhesive lift-off of the latter. Application of a prepatterned adhesive template yields well-defined arrays of reactive epoxide functionality surrounded by a passive fluoropolymer background or vice versa.

KEYWORDS: functional surfaces, surface patterning, nanolayering, plasma deposition, lift-off, adhesion

1. INTRODUCTION

Patterned multifunctional solid surfaces are of importance to a whole variety of technological applications, including thin film transistors,[1] solar cells,[2] genomics,[3−5] proteomics,[6−8] microelectronics,[9−11] sensors,[12] and microfluidics.[13−15] Indeed, a wide range of fabrication methods already exist for such purposes, encompassing shadow masking,[16−19] microcontact printing,[20−27] inkjet printing,[20,28−30] photolithography,[31−35] and scanning probe lithography.[36−42] Each suffers from some drawback, which limits more widespread usage. For instance, microcontact printing requires a favorable combination of interactions between the stamp, the ink, and the substrate;[26] inkjet printing is governed by the trajectory of droplets and their spreading behavior upon surface impact;[29] photolithography often necessitates harsh UV irradiation and significant amounts of chemicals;[20] and scanning probe lithography is a slow, serial technique requiring expensive equipment.[41]

In this article, we outline a simple, solventless approach for fabricating patterned multifunctional surfaces (Scheme 1). The technique entails consecutive plasmachemical deposition of two separate functional nanolayers, followed by selective lift-off of the top passive release layer using a prepatterned adhesive template, in order to expose the underlying bottom active layer.

Plasmachemical nanolayering is already well established as an elegant technique for multilayer functional stack fabrication.[39] Key advantages include no requirement for complex solvent-based surface functionalization chemistries, substrate-independence (metal, inorganic, or polymer substrates), and high-throughput capabilities (e.g., roll-to-roll). Furthermore, pulsed plasma deposited polymer films can be tailored to a high degree of molecular specificity.[43] The short plasma duty cycle on-period (microseconds) generates active sites in the gas phase and at the growing film surface; these initiate conventional polymerization reaction pathways during the longer plasma off-period (milliseconds).[43] By varying the duty cycle, the surface chemistry can be fine-tuned. Specific examples have included anhydride,[43] epoxide,[44] carboxylic acid,[45] amine,[46] cyano,[47] halide,[48] hydroxyl,[49] furfuryl,[50] perfluoroalkyl,[51] and thiol[52] functionalities.

By way of exemplification for the outlined lift-off patterning technique, pulsed plasma deposited poly(glycidyl methacrylate) layers provide reactive epoxide groups,[44] which are amenable to subsequent conventional derivatization reactions with a whole host of functional molecules. The protective release layer constitutes pulsed plasma deposited poly(pentafluorostyrene). Bilayer fabrication entails pulsed plasma polymerization of glycidyl methacrylate (Scheme 2) and then pentafluorostyrene (Scheme 3) immediately afterward, without there being any need to expose the deposited reactive layer to atmospheric conditions inbetween. The lift-off template was prepared by air plasma exposure of adhesive tape through a mask.

2. EXPERIMENTAL SECTION

Polished silicon (100) wafers (Silicon Valley Microelectronics, Inc.) and glass slides (Smith Scientific Ltd.) were used as substrates. Each monomer was loaded into a sealable glass tube and further purified using multiple freeze−pump−thaw cycles. Plasma deposition was carried out in a cylindrical glass chamber pumped by a rotary pump attached to a liquid nitrogen cold trap (base pressure = 4×10^{-3} mbar, leak rate = 2.8×10^{-10} kg s^{-1}). A copper coil wound around the reactor was connected to a 13.56 MHz radio frequency (RF) power supply via an LC matching network. A signal generator was used to trigger the RF power supply. Prior to each deposition, the chamber was cleaned using air plasma (0.2 mbar, 50 W). The substrate to be coated was then placed into the center of the reactor, and the system pumped down to base pressure. Next, precursor vapor was introduced into the chamber at a pressure of 0.2 mbar and a flow rate of 1.6×10^{-7} kg s^{-1}. Following 5 min purging of the reactor, the electrical discharge was ignited.

Received: January 9, 2011
Accepted: March 3, 2011
Published: March 18, 2011

Scheme 1. (a) Bifunctional Patterning Using Glycidyl Methacrylate (Active) and Pentafluorostyrene (Release) Precursors for Plasmachemical Deposition and (b) Pattern Transfer from Adhesive Template to Surface

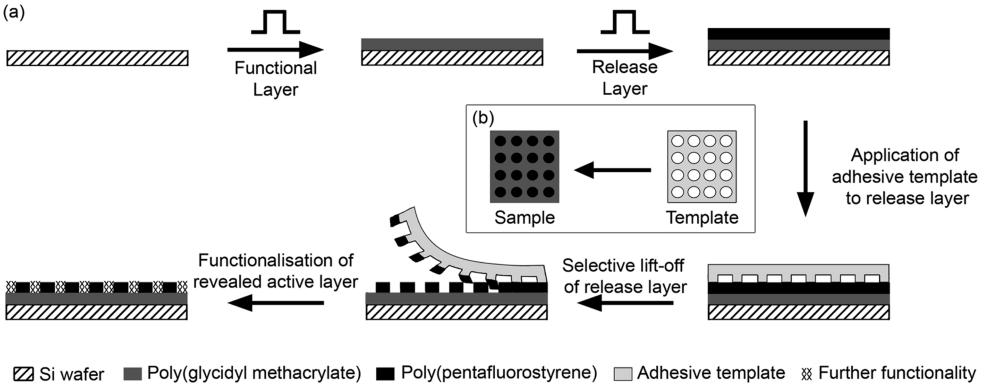

Scheme 2. Structure of Glycidyl Methacrylate

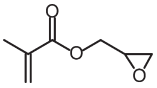

Scheme 3. Structure of Pentafluorostyrene

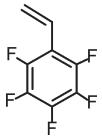

Upon completion of deposition, monomer vapor was allowed to continue to pass through the system for a further 5 min to quench any trapped free radicals in the deposited film, and finally the chamber was pumped down back to base pressure. For bilayer samples, the plasma deposition process was repeated for the second functional layer without exposure of the bottom active layer to the laboratory atmosphere inbetween, Table 1.

A VG ESCALAB spectrometer equipped with an unmonochromatised Mg K_α X-ray source (1253.6 eV) and a concentric hemispherical analyzer (CAE mode, pass energy = 50 eV) was used for X-ray photoelectron spectroscopy (XPS) analysis. The core level spectra were charge referenced to the C(1s) hydrocarbon peak at 285.0 eV and fitted with a linear background and equal full width at half-maximum (fwhm) Gaussian components[53] using Marquardt minimization computer software. Elemental compositions were calculated using sensitivity factors derived from chemical standards: C(1s):O(1s):F(1s) equals 1.00:0.40:0.27.

Fourier transform infrared (FTIR) analysis of the deposited layers was undertaken using a Perkin-Elmer Spectrum One FTIR instrument equipped with a liquid nitrogen cooled MCT detector. Spectra were recorded at a resolution of 4 cm^{-1} across the 700−4000 cm^{-1} wavelength range. Reflection absorption infrared spectroscopy (RAIRS) measurements were performed using a variable angle accessory (Specac) set at 66° and fitted with a KRS-5 polarizer to remove the s-polarized component.

Thickness measurements of films deposited onto silicon wafers were taken using a spectrophotometer (nkd-6000, Aquila Instruments Ltd.). The obtained transmittance−reflectance curves (350−1000 nm wavelength range) were fitted to a Cauchy model for dielectric materials using a modified Levenberg−Marquardt method.[54]

Table 1. Parameters for Pulsed Plasma Deposition

		pulse duty cycle		
monomer	layer	time on	time off	deposition rate, ±4 nm min^{-1}
glycidyl methacrylate (+97%, Sigma-Aldrich)	reactive	20 μs	20 ms	18
pentafluorostyrene (+99%, Sigma-Aldrich)	release	10 μs	50 μs	47
	nonrelease	100 μs	4 ms	23

Peel adhesion tests (ASTM D3359)[55] were carried out for plasma deposited films onto glass substrates. These were pressed against adhesive tape (Scotch Tape 810, 3M) using a force of 5 N for 1 min. The adhesive tape was then manually peeled away from the substrate. For bilayer patterning, the adhesive tape was exposed through a mask to air plasma (30 min, 30 W). This patterned tape was then placed on top of the bilayer and pressed using a force of 5 N for 1 min, followed by manually peeling off the tape.

Fluorescence tagging of epoxide centers associated with patterned poly(glycidyl methacrylate) was accomplished by brief submersion into a 1 mg dm^{-3} aqueous solution of cresyl violet dye (Sigma-Aldrich, Inc.), followed by extensive rinsing with high purity water. Fluorescence microscopy was performed using an Olympus IX-70 system (DeltaVision RT, Applied Precision Inc.). Images were collected using excitation wavelengths at 640 ± 25 nm and emission wavelengths at 685 ± 40 nm, corresponding to the absorption maxima of 633 nm for the cresyl violet dye molecule.

3. RESULTS

(a). Reactive Layer Deposition. XPS analysis of pulsed plasma deposited poly(glycidyl methacrylate) films confirmed the presence of only carbon and oxygen at the surface with no Si(2p) signal detection from the underlying silicon wafer (Table 2). The C(1s) envelope could be fitted to five carbon functionalities:[44] $\underline{C}H$ (285.0 eV), $\underline{C}(CH_3)(C{=}O)O$ (285.85 eV), $O{-}\underline{C}H_2{-}CO$ (286.7 eV), epoxide carbons (287.2 eV), and $\underline{C}(=O)O$ (289.3 eV), which is in good agreement with the structure of glycidyl methacrylate precursor (Figure 1 and Scheme 2).

Infrared spectroscopy of the pulsed plasma deposited film compared favorably with that of the glycidyl methacrylate precursor (Figure 2). For the monomer, the following assignments can be made:[44] epoxide ring C−H stretching (3063 cm^{-1}),

Table 2. XPS Atomic Percentages for Pulsed Plasma Deposited films

functional nanolayer(s)		XPS elemental composition ±0.5%		
		% C	% O	% F
poly(glycidyl methacrylate)				
	theoretical	70.0	30.0	0.0
	experimental	70.2	29.8	0.0
poly(pentafluorostyrene)				
	theoretical	62.0	0.0	38.0
bilayer sample				
nonrelease poly(pentafluorostyrene) (100 μs on, 4 ms off, 30 W)	before lift-off	62.6	2.8	34.6
	after lift-off	61.0	3.0	36.0
release poly(pentafluorostyrene) (10 μs on, 50 μs off, 30 W)	before lift-off	56.4	4.3	39.3
	after lift-off	69.4	30.1	0.5

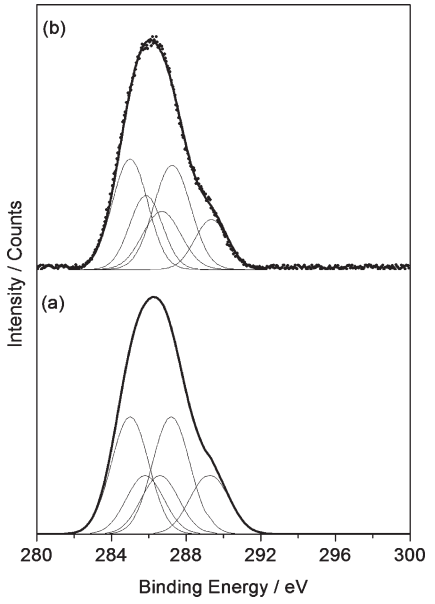

Figure 1. C(1s) XPS spectra and fitted components for poly(glycidyl methacrylate): (a) theoretical curve and (b) pulsed plasma deposited onto silicon wafer (time on = 20 μs, time off = 20 ms, peak power = 30 W).

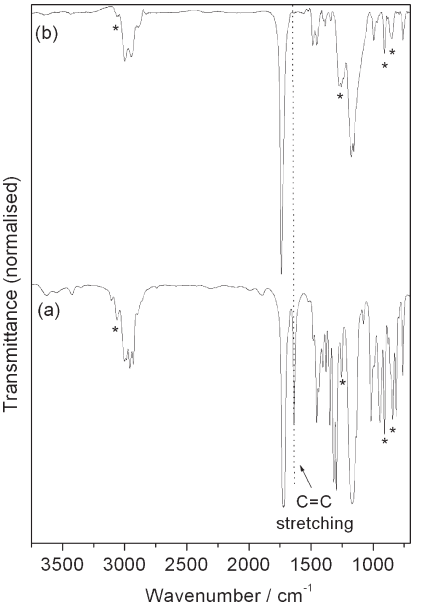

Figure 2. Infrared spectra of (a) glycidyl methacrylate monomer and (b) pulsed plasma deposited film (time on = 20 μs, time off = 20 ms, peak power = 30 W). * Denotes fingerprint epoxide absorbances.

C−H stretching (3000−2900 cm^{-1}), acrylate carbonyl stretching (1735 cm^{-1}), acrylate C═C stretching (1638 cm^{-1}), epoxide ring breathing (1257 cm^{-1}), antisymmetric epoxide ring deformation (909 cm^{-1}), and symmetric ring deformation (850 cm^{-1}). All of these absorbances were evident for the pulsed plasma deposited film, with the exception of the acrylate C═C stretching (1638 cm^{-1}), which is indicative of carbon−carbon bond polymerization proceeding during the prolonged duty cycle off-period.

Peel adhesion tests for pulsed plasma deposited poly(glycidyl methacrylate) films onto glass indicated good adhesion for thicknesses varying between 20−500 nm. The resilience of these layers toward lift-off was confirmed by XPS and infrared analysis.

(b). Release Layer Deposition. Two different duty cycles were utilized for pulsed plasma deposited poly(pentafluorostyrene) films in order to exemplify the degree of control for adhesive behavior: nonrelease (time on = 100 μs, time off = 4 ms, peak power = 30 W, average power = 0.75 W), and slightly harsher conditions for release (time on = 10 μs, time off = 50 μs, peak power = 30 W, average power = 5.0 W). Comparison of the respective XPS C(1s) envelopes indicates a high level of structural retention for the nonrelease film to give good agreement with the theoretical monomer structure:[56,57] CH (285 eV), C−CF (285.8 eV), and CF aromatic (287.6 eV) (Figure 3). More fragmentation/structural rearrangement is noted for the release film leading to carbon functionalities:[56,57] CH (285 eV), C−CF (285.8 eV), CF aromatic (287.6 eV), and also an additional CF nonaromatic (290.5 eV) component fitted to account for the higher binding energy shoulder. These more energetic pulsed plasma deposition conditions were found to give rise to a slightly greater amount of oxygen being detected by XPS (due to more trapped free radicals being capped by oxygen-containing species present in the ambient laboratory atmosphere during transport of the film from the deposition chamber to the XPS spectrometer) (Table 2).

Infrared spectra corresponding to the two pulsed plasma deposition duty cycle regimes were compared with respect to the pentafluorostyrene precursor (Figure 4). Monomer assignments are as follows:[57] vinyl C═C stretching (1648 cm^{-1}), fluorinated aromatic

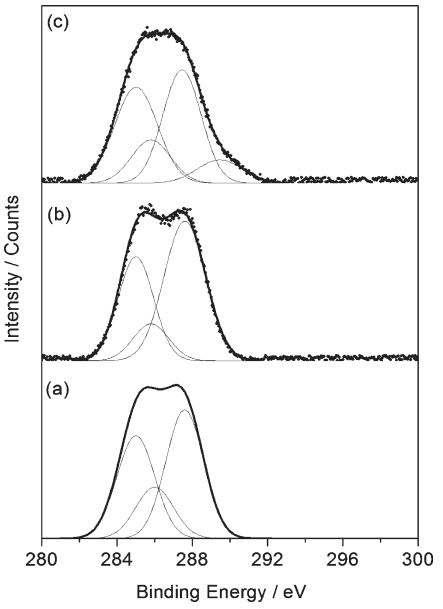

Figure 3. C(1s) XPS spectra and fitted components for poly(pentafluorostyrene): (a) theoretical curve, (b) nonrelease (time on = 100 μs, time off = 4 ms, peak power = 30 W), and (c) release (time on = 10 μs, time off = 50 μs, peak power = 30 W).

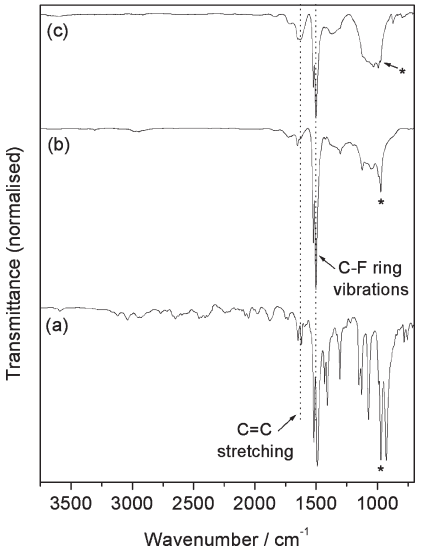

Figure 4. Infrared spectra of (a) pentafluorostyrene monomer, (b) pulsed plasma deposited nonrelease film (time on = 100 μs, time off = 4 ms, peak power = 30 W), and (c) pulsed plasma deposited release film (time on = 10 μs, time off = 50 μs, peak power = 30 W). * Denotes aromatic C−F stretching absorbance.

ring vibrations (1504 cm^{-1}), and C−F (aromatic) stretching (975 cm^{-1}). The sharp vinyl C═C absorbance at 1648 cm^{-1} is absent for both of the plasma deposited films, which is consistent with its role in polymerization. The more energetic duty cycle film displays less structural retention as evident by a drop in the relative signal strength of the perfluorinated aromatic ring absorbance (1504 cm^{-1}) and a general broadening of absorbances.[57] While the much sharper spectral features observed for the milder duty cycle are consistent with a structurally more ordered film structure.

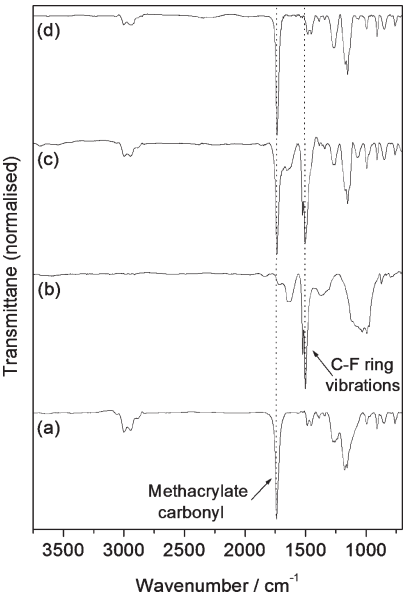

Figure 5. Infrared spectra of (a) pulsed plasma deposited poly(glycidyl methacrylate), (b) more energetic duty cycle pulsed plasma deposited poly(pentafluorostyrene), (c) bilayer sample before lift-off (more energetic duty cycle poly(pentafluorostyrene)/poly(glycidyl methacrylate)), and (d) bilayer sample after lift-off (more energetic duty cycle poly(pentafluorostyrene)/poly(glycidyl methacrylate)).

(c). Lift-Off. Bilayer samples prepared for lift-off adhesion studies comprised pulsed plasma deposited 150 nm thickness poly(pentafluorostyrene) on top of 400 nm thickness poly(glycidyl methacrylate) films. These respective constituents were identifiable by infrared spectroscopy (Figure 5). Tape application followed by lift-off led to the disappearance of the fingerprint perfluorinated aromatic ring features at 975 and 1504 cm^{-1} only in the case of the more energetic duty cycle (greater cross-linking) fluorocarbon layer to leave behind the characteristic bands of the underlying pulsed plasma deposited poly(glycidyl methacrylate) layer.

The greater surface sensitivity of XPS proved beyond all doubt the molecular level chemical specificity of the macroscale lift-off process corresponding to complete removal of the fluorinated release layer. The elemental composition and C(1s) peak shape of the exposed surface closely match those of pulsed plasma deposited poly(glycidyl methacrylate) (Table 2 and Figure 6).

Lift-off pattern transfer to the bottom layer was achieved by using a piece of adhesive tape, which had been exposed to air plasma through a mask in order to create nonadherent regions. The tape was then placed on top of the bilayer sample and peeled off to leave behind an array of pulsed plasma deposited pentafluorostyrene dots (top release layer) surrounded by a background of pulsed plasma deposited glycidyl methacrylate (bottom active layer), which was then tagged with a fluorescent dye (Figure 7).

4. DISCUSSION

The bottom layer of the bilayer assembly is effective because pulsed plasma deposited poly(glycidyl methacrylate) is known to exhibit excellent adhesion to glass, metal, and polymeric substrates.[44] Furthermore, the epoxide groups present can be derivatized following unveiling by lift-off, for example, reaction

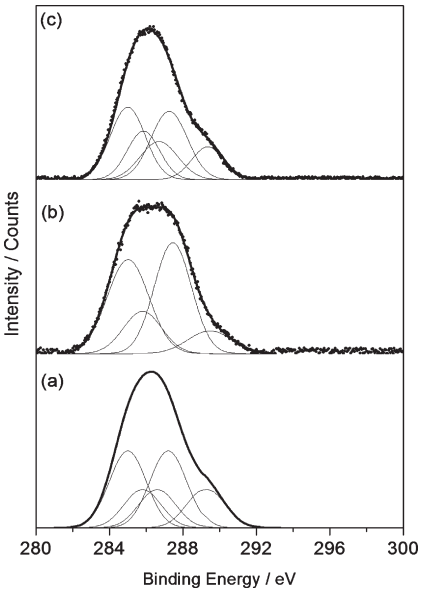

Figure 6. C(1s) XPS spectra and fitted components for (a) theoretical curve for pulsed plasma deposited poly(glycidyl methacrylate), (b) bilayer sample (more energetic duty cycle poly(pentafluorostyrene)/poly(glycidyl methacrylate)) before lift-off, and (c) bilayer sample after lift-off (more energetic duty cycle poly(pentafluorostyrene)/poly(glycidyl methacrylate)).

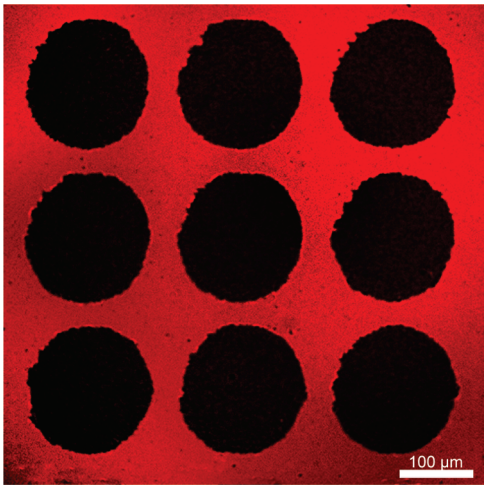

Figure 7. Fluorescence microscopy image of patterned array of pulsed plasma deposited poly(pentafluorostyrene) dots surrounded by a background of pulsed plasma deposited poly(glycidyl methacrylate), which has been derivatized with cresyl violet dye following lift-off.

with nucleophilic reagents[44] for biotechnological applications. Alternatively a whole host of other reactive centers may be utilized by appropriate selection of functional precursor for pulsed plasma-chemical deposition, including anhydride, carboxylic acid, amine, cyano, halide, hydroxyl, thiol, furfuryl, etc.[46−52]

For overall successful operation of the lift-off patterning technique, adhesion at the active layer/substrate interface needs to be stronger than at the active layer/release layer interface. This is accomplished by fine-tuning the pulsed plasma deposition duty cycle for the poly(pentafluorostyrene) top layer to achieve interlayer failure of the tape test[57] (release). Two mechanisms can be postulated for the observed molecular scale lift-off process. On the one hand, it is known that the more energetic pulsing scheme will cause a greater density of trapped free radical species to become incorporated as evident by the increased levels of surface oxygen (Table 2). These could display a greater affinity toward the adhesive tape culminating in lift-off. Alternatively, the greater level of cross-linking in the plasma deposited film could inhibit polymer−polymer interdiffusion across the interface with the underlying layer to enable lift-off with molecular scale precision.

Given the high degree of interlayer molecular specificity demonstrated in the present study and the previously described amenability of plasmachemical deposited functional multilayers for nanolithography,[39] it is envisaged that the outlined lift-off technique could be easily adapted for rapid nanofabrication and roll-to-roll processing. Indeed, it offers several distinct advantages compared to conventional approaches; for instance, in the case of microcontact printing where the transfer of an "ink" material from a patterned stamp to a substrate[20] relies on the ink-substrate interactions being more favorable (stronger) than the ink-stamp interactions, there is an inherent limit on the types of material that can be utilized even with the inclusion of release layers inbetween the stamp and the ink.[26] In contrast for the lift-off technique, pulsed plasma deposition provides a wide range of functional groups in conjunction with excellent adhesion to a large selection of substrates;[46−52] also, there is no requirement for harsh solvents (alleviating the requirement for complex procedures commonly associated with surface device fabrication[33−35]). Another key attribute is protection of the active (bottom) layer at all times by the top release layer prior to patterned lift-off. Given that deposition of both functional layers takes place inside a sealed chamber without the need for interruption to introduce masks or other patterning devices, the overall process offers additional benefits, including sterility, cleanliness, and the scope to preserve highly reactive (air-sensitive) functional groups in the bottom layer right up to the point of application. For instance, patterned pulsed plasma deposited poly(4-vinylpyridine) could be utilized for electroless metallisation,[58] complete with an insulating surround for microelectronics.

5. CONCLUSIONS

Plasmachemical deposited bilayer assemblies comprising an active bottom layer and protective top release layer can be patterned by way of selective lift-off of the top layer using a prepatterned adhesive tape. Such patterned surfaces are amenable to further chemical derivatization of the exposed reactive domains. The outlined approach ensures complete decoupling between pattern creation and subsequent functionalization steps.

REFERENCES

(1) Whang, Z.; Zhang, J.; Xing, R.; Yuan, J.; Yan, D.; Han, Y. *J. Am. Chem. Soc.* **2003**, *125*, 15278.
(2) Jiang, P.; McFarland, M. J. *J. Am. Chem. Soc.* **2005**, *127*, 3710.
(3) Peterlinz, K. A.; Georgiadis, R. M.; Herne, T. M.; Tarlov, M. J. *J. Am. Chem. Soc.* **1997**, *119*, 3401.
(4) Schena, M.; Shalon, D.; Davis, R. W.; Brown, P. O. *Science* **1995**, *270*, 467.
(5) Georgiadis, R.; Peterlinz, K. P.; Peterson, A. W. *J. Am. Chem. Soc.* **2000**, *122*, 3166.
(6) MacBeath, G.; Schreiber, S. L. *Science* **2000**, *289*, 1760.
(7) Kane, R. S.; Takayama, S.; Ostuni, E.; Ingber, D. E.; Whitesides, G. M. *Biomaterials* **1999**, *20*, 2363.
(8) Zhou, H.; Baldini, L.; Hong, J.; Wilson, A. J.; Hamilton, A. D. *J. Am. Chem. Soc.* **2006**, *128*, 2421.

(9) Zhong, Z.; Wang, D.; Cui, Y.; Bockrath, M. W.; Lieber, C. M. *Science* **2003**, *302*, 1377.
(10) Filho, F. H. D.; Mauricio, M. H. P.; Ponciano, C. R.; Prioli, R. *Mater. Sci. Eng., B* **2004**, *112*, 194.
(11) Wallraff, G. M.; Hinsberg, W. D. *Chem. Rev.* **1999**, *99*, 1801.
(12) Wei, C.; Dai, L.; Roy, A.; Tolle, T. B. *J. Am. Chem. Soc.* **2006**, *128*, 1412.
(13) Kline, R. T.; Paxton, F. W.; Wang, Y.; Velegol, D.; Mallouk, T. E.; Sen, A. *J. Am. Chem. Soc.* **2005**, *127*, 17150.
(14) Beebe, D. J.; Moore, J. S.; Yu, Q.; Liu, R.; Kraft, M. L.; Jo, B.; Devadoss, C. *Proc. Natl. Acad. Sci. U.S.A.* **2000**, *97*, 13488.
(15) Beebe, D. J.; Mensing, G. A.; Walker, G. M. *Ann. Rev. Biomed. Eng.* **2002**, *4*, 261.
(16) Tixier, A.; Mita, Y.; Gouy, J. P.; Fujita, H. *J. Micromech. Microeng.* **2000**, *10*, 157.
(17) Yoshimura, T.; Terasawa, N.; Kazama, H.; Naito, Y.; Suzuki, Y.; Asama, K. *Thin Solid Films* **2006**, *497*, 182.
(18) Duffy, D. C.; Jackman, R. J.; Vaeth, K. M.; Jensen, K. F.; Whitesides, G. M. *Adv. Mater.* **1999**, *11*, 546.
(19) Ostuni, E.; Kane, R.; Chen, C. S.; Ingber, D. E.; Whitesides, G. M. *Langmuir* **2000**, *16*, 7811.
(20) Nie, Z.; Kumacheva, E. *Nat. Mater.* **2008**, *7*, 277.
(21) Park, J.; Kim, Y. S.; Hammond, P. T. *Nano Lett.* **2005**, *5*, 1347.
(22) Zhou, F.; Zheng, Z. J.; Yu, B.; Liu, W. M.; Huck, W. T. S. *J. Am. Chem. Soc.* **2006**, *128*, 16253.
(23) Kumar, A.; Whitesides, G. M. *Appl. Phys. Lett.* **1993**, *63*, 2002.
(24) Rogers, J. A.; Bao, Z.; Baldwin, K.; Dodabalapur, A.; Crone, B.; Raju, V. R.; Kuck, V.; Katz, H.; Amundson, K.; Ewing, J.; Drzaic, P. *Proc. Natl. Acad. Sci. U.S.A.* **2001**, *98*, 4835.
(25) Bernard, A.; Renault, J. P.; Michel, B.; Bosshard, H. R.; Delamarche, E. *Adv. Mater.* **2000**, *12*, 1067.
(26) Schvartzman, M.; Mathur, A.; Hone, J.; Jahnes, C.; Wind, S. J. *Appl. Phys. Lett.* **2008**, *93*, 153105.
(27) Hui, C. Y.; Jagota, A.; Lin, Y. Y.; Kramer, E. J. *Langmuir* **2002**, *18*, 1394.
(28) Shimoda, T.; Morii, K.; Seki, S.; Kiguchi, H. *Mater. Res. Soc. Bull.* **2003**, *28*, 821.
(29) Sirringhaus, H.; Kawase, T.; Friend, R. H.; Shimoda, T.; Inbasekaran, M.; Wu, W.; Woo, E. P. *Science* **2000**, *290*, 2123.
(30) Kröber, P.; Delaney, J. T.; Perelaer, J.; Schubert, U. S. *J. Mater. Chem.* **2009**, *19*, 5234.
(31) Drury, C. J.; Mutsaers, M. J.; Hart, C. M.; Matters, H. M.; de Leeuw, D. M. *Appl. Phys. Lett.* **1998**, *73*, 108.
(32) Reichmanis, E.; Roman, B. J.; Tai, K. L.; Wilkins, J. C. W. U. S. Pat. No. 4,373,018, 1983.
(33) Ilic, B.; Craighead, H. G. *Biomed. Microdevices* **2000**, *2*, 317.
(34) Craighead, H. G.; Ilic, B. U. S. Patent 6,559,474, 2003.
(35) Liu, S.; Becerril, H. A.; LeMieux, M. C.; Wang, W. M.; Oh, J. H.; Bao, Z. *Adv. Mater.* **2009**, *21*, 1266.
(36) Gates, B. D.; Xu, Q.; Stewart, M.; Ryan, D.; Willson, C. G.; Whitesides, G. M. *Chem. Rev.* **2005**, *105*, 1171.
(37) Piner, R. D.; Zhu, J.; Xu, F.; Hong, S.; Mirkin, C. A. *Science* **1999**, *283*, 661.
(38) Xu, S.; Miller, S.; Laibinis, P. E.; Liu, G. *Langmuir* **1999**, *15*, 7244.
(39) Harris, L. G.; Schofield, W. C. E.; Badyal, J. P. S. *Chem. Mater.* **2007**, *19*, 1546.
(40) Headrick, J. E.; Armstrong, M.; Cratty, J.; Hammond, S.; Sheriff, B. A.; Berrie, C. L. *Langmuir* **2005**, *21*, 4117.
(41) Minne, S. C.; Adams, J. D.; Yaralioglu, G.; Manalis, S. R.; Atalar, A.; Quate, C. F. *Appl. Phys. Lett.* **1998**, *73*, 1742.
(42) Hong, S.; Mirkin, C. A. *Science* **2000**, *288*, 1808.
(43) Ryan, M. E.; Hynes, A. M.; Badyal, J. P. S. *Chem. Mater.* **1996**, *8*, 37.
(44) Tarducci, C.; Kinmond, E. J.; Badyal, J. P. S.; Brewer, S. A.; Willis, C. *Chem. Mater.* **2000**, *12*, 1884.
(45) Hutton, S. J.; Crowther, J. M.; Badyal, J. P. S. *Chem. Mater.* **2000**, *12*, 2282.
(46) Harris, L. G.; Schofield, W. C. E.; Doores, K. J.; Davis, B. G.; Badyal, J. P. S. *J. Am. Chem. Soc.* **2009**, *131*, 7755.
(47) Tarducci, C.; Schofield, W. C. E.; Brewer, S.; Willis, C.; Badyal, J. P. S. *Chem. Mater.* **2001**, *13*, 1800.
(48) Teare, D. O. H.; Barwick, D. C.; Schofield, W. C. E.; Garrod, R. P.; Ward, L. J.; Badyal, J. P. S. *Langmuir* **2005**, *21*, 11425.
(49) Tarducci, C.; Schofield, W. C. E.; Brewer, S. A.; Willis, C.; Badyal, J. P. S. *Chem. Mater.* **2002**, *14*, 2541.
(50) Tarducci, C.; Brewer, S. A.; Willis, C.; Badyal, J. P. S. *Chem. Commun.* **2005**, *3*, 406.
(51) Coulson, S. R.; Woodward, I. S.; Badyal, J. P. S.; Brewer, S. A.; Willis, C. *Chem. Mater.* **2000**, *12*, 2031.
(52) Schofield, W. C. E.; McGettrick, J.; Bradley, T. J.; Badyal, J. P. S.; Przyborski, S. *J. Am. Chem. Soc.* **2006**, *128*, 2280.
(53) Evans, J. F.; Gibson, J. H.; Moulder, J. F.; Hammond, J. S.; Goretzki, H. *Fresenius, J. Anal. Chem.* **1984**, *319*, 841.
(54) Tabet, M. F.; McGahan, W. A. *Thin Solid Films* **2000**, *370*, 122.
(55) Standard Test Methods for Measuring Adhesion by Tape Test; ASTM Standard D3359 09e2; ASTM International: West Conshohocken, PA, 2003, DOI: 10.1520/D3359-09E02, www.astm.org.
(56) Beamson, G.; Briggs, D. *High Resolution XPS of Organic Polymers*; John Wiley & Sons: New York, 1992; p 278.
(57) Han, L. M.; Timmons, R. B.; Lee, W. W.; Chen, Y.; Hu, Z. *J. Appl. Phys.* **1998**, *84*, 439.
(58) Bradley, T. J.; Schofield, W. C. E.; Garrod, R. P.; Badyal, J. P. S. *Langmuir* **2006**, *22*, 7552.